



This is a repository copy of *The effect of dispersion condition on the structure and properties of polystyrene/graphene oxide nanocomposites*.

White Rose Research Online URL for this paper:  
<https://eprints.whiterose.ac.uk/167742/>

Version: Accepted Version

---

**Article:**

Mohammadsalih, Z.G., Inkson, B.J. [orcid.org/0000-0002-2631-9090](https://orcid.org/0000-0002-2631-9090) and Chen, B. (2021) The effect of dispersion condition on the structure and properties of polystyrene/graphene oxide nanocomposites. *Polymer Composites*, 42 (1). pp. 320-328. ISSN 0272-8397

<https://doi.org/10.1002/pc.25827>

---

This is the peer reviewed version of the following article: Mohammadsalih, ZG, Inkson, BJ, Chen, B. The effect of dispersion condition on the structure and properties of polystyrene/graphene oxide nanocomposites. *Polymer Composites*. 2021; 42: 320– 328, which has been published in final form at <https://doi.org/10.1002/pc.25827>. This article may be used for non-commercial purposes in accordance with Wiley Terms and Conditions for Use of Self-Archived Versions. This article may not be enhanced, enriched or otherwise transformed into a derivative work, without express permission from Wiley or by statutory rights under applicable legislation. Copyright notices must not be removed, obscured or modified. The article must be linked to Wiley's version of record on Wiley Online Library and any embedding, framing or otherwise making available the article or pages thereof by third parties from platforms, services and websites other than Wiley Online Library must be prohibited.

**Reuse**

Items deposited in White Rose Research Online are protected by copyright, with all rights reserved unless indicated otherwise. They may be downloaded and/or printed for private study, or other acts as permitted by national copyright laws. The publisher or other rights holders may allow further reproduction and re-use of the full text version. This is indicated by the licence information on the White Rose Research Online record for the item.

**Takedown**

If you consider content in White Rose Research Online to be in breach of UK law, please notify us by emailing [eprints@whiterose.ac.uk](mailto:eprints@whiterose.ac.uk) including the URL of the record and the reason for the withdrawal request.



[eprints@whiterose.ac.uk](mailto:eprints@whiterose.ac.uk)  
<https://eprints.whiterose.ac.uk/>

## **The effect of dispersion condition on the structure and properties of polystyrene/graphene oxide nanocomposites**

**Zaid G. Mohammadsalih<sup>a</sup>, Beverley J. Inkson<sup>b</sup> and Biqiong Chen<sup>c,\*</sup>**

<sup>a</sup>Applied Science Research Unit, Applied Science Department, The University of Technology, Baghdad, Iraq.

<sup>b</sup>Department of Materials, University of Sheffield, Mappin Street, Sheffield, S1 4NS, U.K.

<sup>c</sup>School of Mechanical and Aerospace Engineering, Queen's University Belfast, Stranmillis Road, Belfast, BT9 5AH, U.K.

\*Correspondence: Author Email Address: [b.chen@qub.ac.uk](mailto:b.chen@qub.ac.uk)

### **Abstract**

The realization of an optimum strategy for dispersing graphene nano-sheets in a thermoplastic matrix is important for obtaining a successful preparation and, consequently, a better enhancement of different properties for the resultant polymer/graphene nanocomposites. In this study, nanocomposites of polystyrene (PS) and graphene oxide (GO) were prepared using solution blending method with tetrahydrofuran as the solvent. Magnetic stirring, water bath sonication, and shear mixing were utilised to disperse GO nano-sheets in PS. Different periods of mixing for the last two techniques were examined to study their effect on the structure and properties on the PS/GO nanocomposites. For the 1<sup>st</sup> sample, water bath sonication and shear mixing were used for 30 and 60 minutes respectively. For the 2<sup>nd</sup> sample, both mixing periods were doubled. The results obtained by employing different characterization techniques showed a good dispersion of nano-sheets in the matrix and enhanced thermal and thermo-mechanical properties for both samples, with a superiority for the 1<sup>st</sup> sample in terms of storage modulus to prevent the nano-sheets from damage due to the application of sonication and mixing for a shorter period of time.

**Keywords: Polystyrene, Graphene Oxide, Dispersion.**

## Introduction

Polystyrene (PS) is one of the most widely used commodity polymers due to the convenience of its processing as well as its relatively good chemical resistance, low density, and high performance / price ratio <sup>[1]</sup>. Graphene and its derivatives are promising fillers to prepare polymer nanocomposites that have prosperous horizons in both technologies and applications <sup>[2]</sup>. Graphene is one of allotropes of elemental carbon that is composed of sp<sup>2</sup> hybridized carbon atoms <sup>[3]</sup>. It is a 2D honeycomb lattice with a planar monolayer of carbon atoms. It has exceptional properties such as high Young's modulus (1 TPa), high electron mobility ( $\sim 200,000 \text{ cm}^2 \text{ V}^{-1} \text{ S}^{-1}$ ) at room temperature and superior thermal conductivity ( $5000 \text{ W m}^{-1} \text{ K}^{-1}$ ) <sup>[4, 5]</sup>. The high cost of the high quality graphene production still represents a barrier towards obtaining a real booming in the field, which explains the reason behind the employment of wet chemistry to obtain exfoliated graphene by the oxidation of graphite that results in graphene oxide (GO) <sup>[6]</sup>. Graphene oxide can be defined as an atomic sheet of graphite which is a single layer material that possesses a high surface area and is decorated by oxygenated functional groups on both the edges and the basal planes <sup>[7, 8]</sup>.

The common definition for polymer nanocomposites is the efficient combination of polymer matrices with the additives that have at least one dimension in the nanometre scale <sup>[9]</sup>. Some researchers <sup>[10]</sup> found a significant improvement of the mechanical properties such as the Young's modulus improved to 10 times and tensile strength improved by 150% for poly(vinyl alcohol)/graphene nanocomposites containing 1.8 vol.% fully exfoliated and randomly dispersed graphene nano-sheets compared to the values of its polymer matrix. The improvement in the physical and mechanical properties of polymer nanocomposite is intimately associated with a good dispersion of the nano-filler in the matrix. This improvement is linked to both the synthesis and processing techniques, as reported in the literature <sup>[11]</sup>.

To date, three main approaches have been used to prepare polymer/graphene oxide nanocomposites: solution blending, *in-situ* polymerization and melt processing. The first two approaches have often resulted in a good dispersion of nano-additives in the polymer matrices. On the other hand, melt processing approach is largely used in plastic industry but the dispersion of nano-additives in the polymer matrices using this approach is relatively poor [12]. In the case of solution blending, the full exploitation for the physical and mechanical properties of polymer nanocomposites requires an appropriate selection of the solvent, organic or aqueous medium. A good dispersion of the nano-additive in the matrix should also have adequate stability in the resulting nanocomposite [13].

For instance, some researchers [14] found that better dispersion and high stability for graphene sheets in poly(vinyl chloride) were obtained by the use of tetrahydrofuran. By ensuring a well dispersed system the interfacial surface area will be maximized, which means that the neighbouring polymer chains are immobilized on the nano-sheets' surface and hence the properties for the whole nanocomposite will be enhanced [15, 16]. Other researchers [17] found that poor dispersion of graphene in polymer matrices led to poor performance for nanocomposites with limited applications. The indispersibility of graphene in most solvents can be considered as one of the most prominent limitations for the real-life application of this material [18].

A number of parameters have to be considered to ensure a good dispersion of nano-particles. For example, energy barrier should be present to prevent aggregation and this can be achieved by either steric repulsion or electrostatic repulsion. In case of high energy barrier, Brownian motion will play a major role for dispersion maintenance. This can be reached by graphene modification either covalently or non-covalently and by appropriate selection for the solvent [13].

In addition, there are many other contributing factors that may help in tackling the challenges related to the manufacture process of polymer nanocomposites. Among these is the use of more scalable routes for dispersion, such as, shear mixing [13]. For example, some authors [11] concluded that the best modulus enhancement for epoxy reinforced with expanded graphite can be achieved with the aid of shear mixing rather than other dispersion technique such as direct magnetic stirring or sonication.

Graphene oxide has many functional groups that make it hydrophilic and help form a highly dispersible graphene oxide in the aqueous medium [19]. The electrostatic repulsion between the negatively charged sheets confirmed by the negative Zeta potential (- 64 mV) is the main cause of having a stable aqueous GO suspension at its equilibrium state [20]. Different macroscopic materials can be processed using a stable colloidal dispersion of GO such as composites, coatings and thin films [21].

Superior properties for polymer nanocomposites cannot be achieved without a good dispersion of nano-particles in the matrix. As described above, the benefits of homogenous dispersion of nano-particles in the polymer matrix are to maximise the available matrix-particle interface and hence the interfacial interactions. Dedicated scientific efforts are focusing on the development and promotion of the rational processing strategies of nanocomposite materials that lead to the enhancement of particle-matrix interactions.

Solution blending is a simple strategy to prepare polymer nanocomposites. It includes four major steps: dispersion of the nano-particles in a suitable solvent using a specific technique such as sonication, the addition of the polymer solution, further mixing, and finally solvent removal by evaporation or distillation [16]. Noteworthy, during solution blending the quality of dispersion can be affected by the mixing equipment, mixing velocity, and mixing time [22].

Some studies have indicated that the combination of dispersion techniques such as ultrasonication and shear mixing leads to a good dispersion of nano-particles in the polymer matrix [23, 11]. For instance, some studies [24] investigated the dispersion homogeneity of carbon nano-fibres in the epoxy matrix by dispersing the nano-fibres in chloroform and using several techniques, including direct magnetic stirring, sonication, and high shear mixing, to ensure homogenous dispersion of the nano-fibres in the epoxy resin before curing. Another research group [25] who studied the role of shear speed in the uniform dispersion of the nano-fillers in epoxy resin found that a higher speed led to better dispersion and that the optimal speed was 1500 rpm for 10 minutes. They also mentioned that only 20% of researchers used the shear mixer for longer for up to one or two hours and employing it for longer time led to an increased temperature with a possibility of damaging the nano-fillers.

This research aimed to investigate the effect of mixing time on the structure and properties of the polymer/graphene oxide nanocomposites. An improved Hummers' method was used to prepare graphene oxide [26], and solution blending method was used to prepare PS/GO nanocomposites. The weight fraction of GO used with the polymer matrix was 0.5 wt. % which was considered to be an appropriate loading for engineering applications [27]. Two different dispersion techniques, namely bath sonication and shear mixing, were employed successively for different periods and their impact on the structure and properties was investigated.

## **Experimental**

### **Materials**

Pellets of polystyrene (Styron 634, Dow Chemical Company) were obtained from RESINEX, UK. Graphite powder with a lateral size of  $\leq 20 \mu\text{m}$  was from Sigma Aldrich, UK. Other chemicals had a purity that is mentioned with each item: potassium permanganate (97%),

sodium nitrate (>99%), sulphuric acid (95-98 %), hydrochloric acid (36.5%) in water, hydrogen peroxide (29 – 32 %) in H<sub>2</sub>O, and tetrahydrofuran (THF, >99.5%). All these chemicals were purchased from Sigma Aldrich, UK.

### **Preparation of graphite oxide, graphene oxide and PS/GO nanocomposites**

An improved Hummer's method was used to prepare graphite oxide according to Marcano et al. [26]. 6 g of graphite was mixed with 3 g of NaNO<sub>3</sub> in a beaker. 138 ml of high concentrated H<sub>2</sub>SO<sub>4</sub> (98%) was added to the beaker which was put in an ice bath to keep the reaction temperature below 35 °C. Then, 36 g of KMNO<sub>4</sub> was added gradually over 2 days. A magnetic stirrer was used to mix these chemicals at a speed of 200 rpm. A yellow brown viscous mixture was obtained. 10-15 ml of H<sub>2</sub>O<sub>2</sub> was added to quench the reaction [28]. 400 ml of distilled water and 100 ml of HCL were mixed in a test tube and used for washing the graphite oxide to eliminate the acidity of the solution. Centrifugation (Richmond Scientific Limited, UK and Eppendorf, Germany) was performed at 8000 rpm for 1 hour each time and the graphite oxide was washed with distilled water over 18 h till the pH of the suspension reached 5.5. The obtained suspension of graphite oxide was sonicated for 1 h by a bath sonicator (Fisher brand Elma, Germany) and centrifuged for 30 minutes at 6000 rpm. The suspension was casted into Teflon coated metal tray and left to freeze in a freezer for 24 h at -40 °C. GO then was placed inside the chamber of a freeze drying machine (Bradley Refrigeration, Edwards, UK) for 48 hours under a pressure around 10<sup>-1</sup> bar. Finally, GO was obtained as a fluffy powder material.

The nanocomposites samples were prepared using THF with two different procedures. 20 g of PS pellets were dissolved in 200 ml of THF magnetic stirring for 2 h at 600 rpm. 100 mg of GO was stirred in 100 ml of THF for 2 h at 600 rpm and sonicated for 30 minutes to prepare GO/THF suspension. The GO/THF suspension was added to the PS/THF solution at the weight percentages of GO in PS/GO nanocomposites of 0 and 0.5 %, which was stirred for 90 minutes

using a magnetic stirrer, followed by 30 minutes of bath sonication and 60 minutes of shear mixing (Silverson, UK) at 1600 rpm/Amp 0.3.

In the second case, longer time of sonication and shear mixing was investigated. Bath sonication was used for 60 minutes and shear mixer was used for 120 minutes, which means that both mixing periods were doubled to study their effect on the structure and properties of the nanocomposites. The obtained suspension of PS/GO was poured in glass covered Petri-dishes to ensure a slow evaporation of the solvent. All samples were left to dry in a fume cupboard for 1 week and then in vacuum oven for 3 hours at 40 °C.

The first sample prepared was denoted to as PS/GO (ordinary mixing time) while the second one was referred to as PS/GO D (double mixing time for bath sonication and shear mixing).

## **Characterization**

Scanning Electron Microscopy (SEM Inspect F, Poland) was used to characterize GO and the fracture surface for the samples at 10 kV. Samples were coated manually with silver dag followed by gold coating for 3 minutes using a sputter coater machine (Emscope SC 500, England).

The optical microscopy (Swift, New York Microscope Co. USA) was utilized for imaging the PS/GO and PS/GO D samples to establish a basic indication for the distribution of GO in PS matrix. To further investigate the quality of dispersion of the nano-sheets in the matrix, transmission electron microscopy (TEM) was used. Sample of PS/GO 0.5 wt. % was snapped frozen in liquid nitrogen and placed in the FC6 cryo chamber to equilibrate for around 30 minutes. Ultrathin sections, approximately 90-100 nm thick, were cut using a Leica UC 6 ultra-microtome and FC6 cryo-box attachment onto uncoated 200 mesh copper grids at temperatures of between -60 to -100 °C. Sections were examined using a FEI Tecnai TEM at an accelerating



voltage of 80 kV or 100 kV. Electron micrographs were recorded using a Gatan Orius camera and Gatan digital micrograph software.

Fourier Transform Infrared Spectroscopy (FTIR, Spectrum 100 Perkin Elmer, USA) was utilised with the range of 400-4000  $\text{cm}^{-1}$ . The resolution of 4  $\text{cm}^{-1}$  was used for characterizing GO, PS and PS/GO nanocomposites. The number of scans used to obtain the spectra was 16 scans, and the scan speed was 0.2  $\text{cm}\cdot\text{sec}^{-1}$ . The used source attached to the machine was MIR 8000-30  $\text{cm}^{-1}$  and the detector was MIR TGS 15000-370  $\text{cm}^{-1}$ .

Thermal Gravimetric Analysis (TGA Pyris 1, Perkin Elmer, USA) was used to measure thermal degradation temperature of the materials. The atmosphere of the test was  $\text{N}_2$  with a flow rate of 50  $\text{ml}\cdot\text{min}^{-1}$ , and the heating rate was 10  $^\circ\text{C}\cdot\text{min}^{-1}$ . The range of temperature that used with GO and PS/GO nanocomposites was from 28 to 600  $^\circ\text{C}$ .

Differential Scanning Calorimetry (DSC 6 Perkin Elmer, USA) was used to find out the value of glass transition temperature  $T_g$ . The weight of the samples used in this experiment was 10 mg placed in a sealed pan of aluminium with an empty sealed aluminium pan used as a reference. Both of the sample and the reference were put inside the machine under nitrogen gas purging at a rate of 50  $\text{ml}\cdot\text{min}^{-1}$ . The range of temperature was ramped from 25  $^\circ\text{C}$  to 240  $^\circ\text{C}$  at a rate of 10  $^\circ\text{C}\cdot\text{min}^{-1}$  then the latter rate was used to cool the system down to 25  $^\circ\text{C}$  and the temperature went up again to 240  $^\circ\text{C}$  at the same rate as the 2<sup>nd</sup> cycle of heating where  $T_g$  was taken from this curve. The 1<sup>st</sup> cycle was intended to remove the thermal history for the samples.

Dynamic Mechanical Analysis (DMA Perkin Elmer, DMA 8000, USA) was used to find the storage modulus, loss factor ( $\tan \delta$ ), and  $T_g$  for the neat polymer and nanocomposites where strain was 0.5 %, the range of temperature was 30–120  $^\circ\text{C}$ , the heating rate was 3  $^\circ\text{C}\cdot\text{min}^{-1}$  and the oscillatory frequency was 1 Hz.

## Results and discussion

The GO material showed a good dispersion in THF after 30 minutes of bath sonication and 120 minutes of magnetic stirring. Both GO and THF have a relatively high surface energy (62 mN.m<sup>-1</sup> and 26.4 mN.m<sup>-1</sup> respectively), so THF is a good solvent to obtain a stable suspension of GO nano-particles<sup>[29]</sup>. Besides, THF is also considered as a good solvent for PS. The mixing techniques employed in this work led to stable mixtures of GO suspension and PS solution in THF before drying.

The SEM image of the top surface of pristine GO nano-sheets (figure 1 a) shows that the surface had a wrinkled morphology<sup>[30]</sup>. Figure 1 b, c shows the optical micrographs for the PS/GO and PS/GO D nanocomposites prepared by THF. A relatively good distribution for the GO nano-sheets (shown as dark lines) can be seen in the PS matrix for both samples prepared by the two ways of mixing.

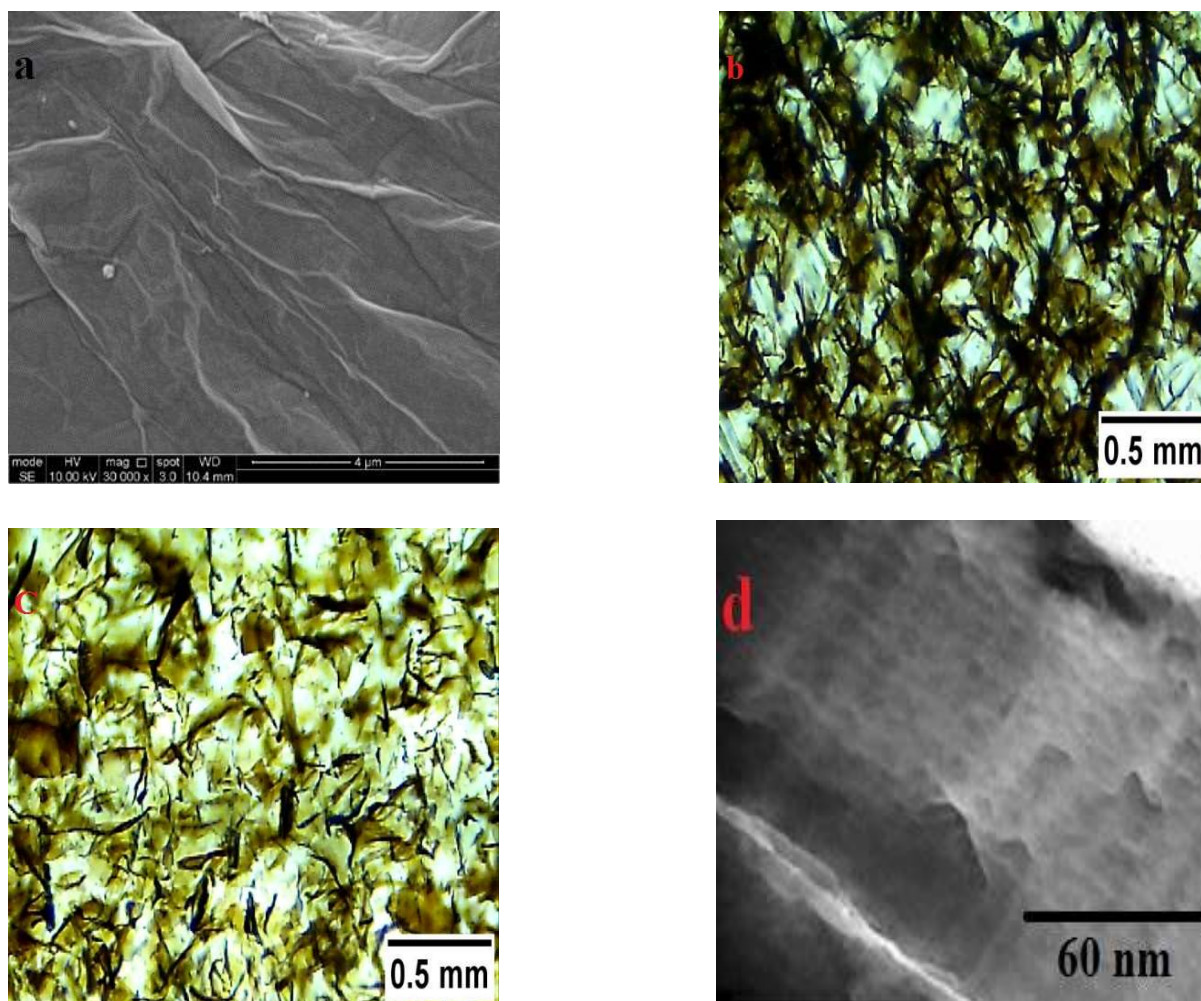


Figure 1: (a) SEM image shows the wrinkled morphology of GO. (b, c) optical micrographs of PS/GO and PS/GO D respectively, and (d) TEM image of PS/GO, shows the dispersion of GO nano-sheets in the PS.

The TEM image in figure 1d shows the fine dispersion of the GO flakes in PS matrix. No aggregations were found in the region. The flakes were curvy and looked like black strips and most of them appeared as single sheets of GO finely dispersed in the matrix that had a grey background. The curvy and individual sheets of GO were also reflected the fact that the flakes had wrinkled morphology and they were exfoliated in the PS. The TEM image from the literature <sup>[31]</sup> of polysulfone (PSF)/GO 0.5 wt. % showed the homogenous dispersion of single sheets GO on the PSF matrix with hardly any aggregations, similar to what is achieved in the current study. They used a continuous stirring for long time (24 h) followed by sonication for 60 minutes, with dimethylformamide as the solvent.

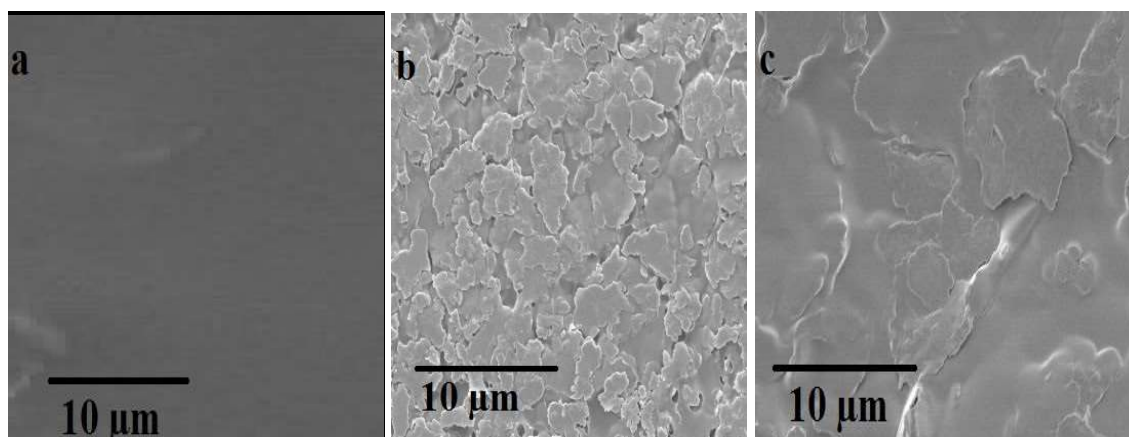


Figure 2: SEM images of (a) PS, (b, c) PS/GO and PS/GO D, respectively.

The SEM images in figure 2 show the fracture surface for neat PS and its nanocomposites that were prepared in two different mixing times. A smooth fracture surface for PS can be seen in figure 2a, whilst the fractography for the nanocomposites in figure 2b and 2c showed rough surfaces. GO nano-sheets embedded in the polymer matrix played a major role in inducing the rough and wrinkled surfaces of the nanocomposites. Moreover, the images of the nanocomposites showed that no obvious aggregations can be seen in the dense regions confirming the results of optical and TEM micrographs.

The FTIR spectrum for GO can be seen in figure 3, along with the spectra of neat polymer and nanocomposites for different times of mixing. For GO spectrum, hydroxyl, epoxide and carboxylic acid represented a rich collection of absorption bands. The O-H stretching vibration appeared at  $3500\text{ cm}^{-1}$ . The range for the O-H stretching vibration appeared at  $3000\text{-}3600\text{ cm}^{-1}$ . C=O stretching vibrations can be seen at  $1730\text{ cm}^{-1}$  which were assigned to carbonyl and carboxylic acid groups as the range for this vibrations is  $1730\text{-}1706\text{ cm}^{-1}$ . The sharp peak of  $1625\text{ cm}^{-1}$  can be attributed to the unoxidized graphitic domain. This domain can be found within the range of  $1680\text{-}1450\text{ cm}^{-1}$  which is attributed to the remaining C=C in GO. C-H bending vibration was located at  $1340\text{ cm}^{-1}$ , which had a range of  $1465\text{-}1340\text{ cm}^{-1}$ . The sharp peak at  $1045\text{ cm}^{-1}$  and the weak peak at  $1238\text{ cm}^{-1}$  were related to C-O stretching vibrations, the former of which represented the epoxy groups. C-O stretching vibrations have a range of  $1300\text{-}$

1000  $\text{cm}^{-1}$ . The hydrophilicity of GO was ascribed to the abundance of these oxygenated functional groups [32, 33]. Some authors [34] reported the presence of OH, C=O and C-O groups in their sample of GO at quite similar wavenumbers compared with GO in the current study.

The peaks at the following wavenumbers 3025, 2923, 1492, 1452 and 698  $\text{cm}^{-1}$  were related to PS. The shoulders of 2923 and 3025  $\text{cm}^{-1}$  were attributed to the presence of C-H stretching vibration of the aliphatic chain and aromatic ring, respectively. The peaks of 1452 and 1492  $\text{cm}^{-1}$  represented the C-C stretching of benzene ring. The peak located at 1023  $\text{cm}^{-1}$  of C-C group in the FTIR spectra could be related to PS benzene. Some researchers [35] reported a peak of benzene that is related to PS structure located at 1027  $\text{cm}^{-1}$  whilst other researchers [36] reported a peak located at 1028  $\text{cm}^{-1}$  which was also classified as an intrinsic peak of PS. The other main peaks related to PS; apart of those highlighted by dash lines in figure 3; were located at 753, 1600, and 2849  $\text{cm}^{-1}$ . These peaks were assigned to C-H out of plane bending vibration of benzene ring, stretching vibration of benzene ring, and symmetric stretching vibration of  $\text{CH}_2$ , respectively. The majority of peaks for PS were presented in the samples of nanocomposites of different times of mixing with no obvious peak related to GO which can be ascribed to its low content in the nanocomposites [1, 33, 37].

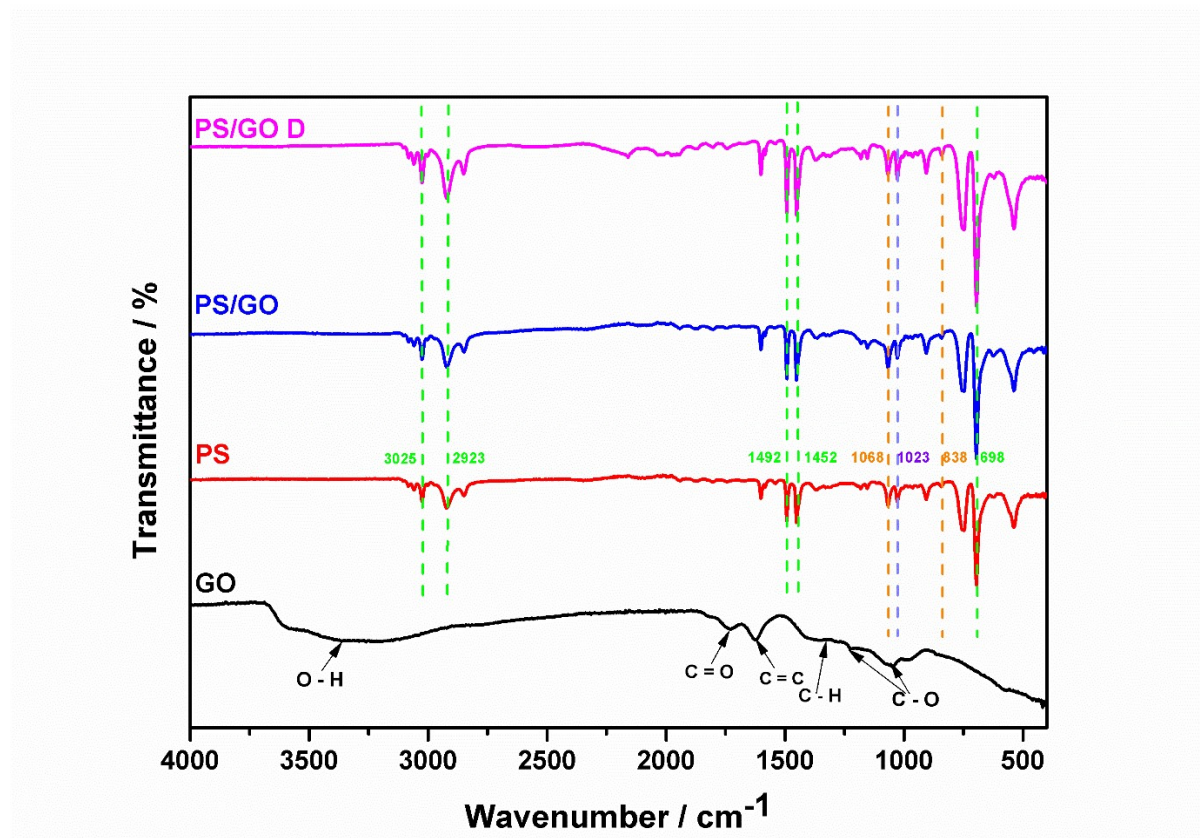


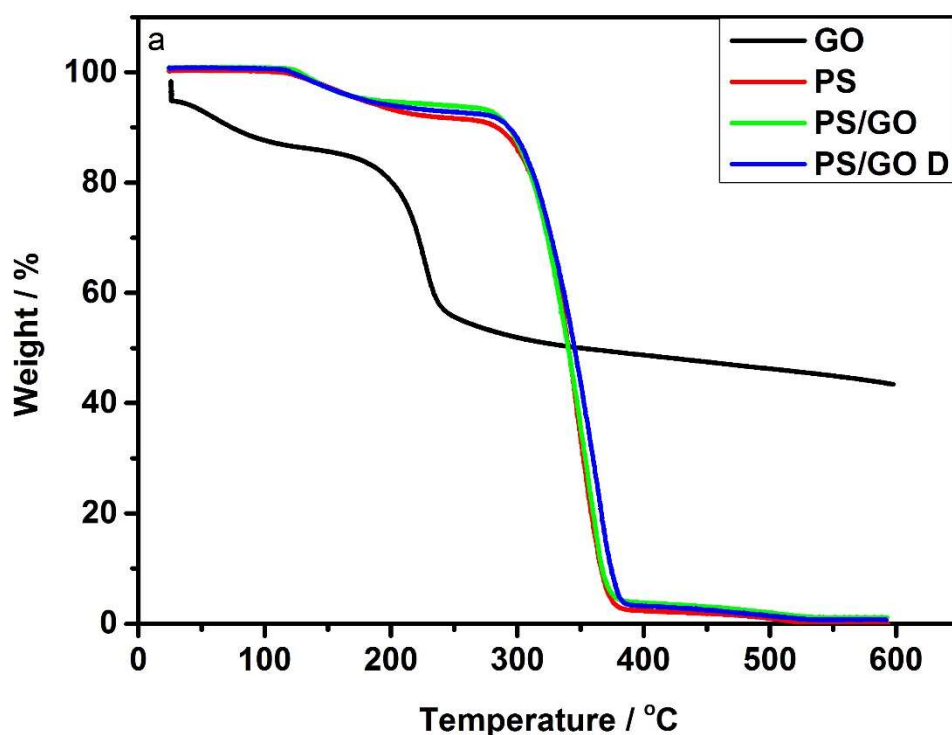
Figure 3: FTIR peaks for GO, PS and PS/GO for different periods of mixing.

The TGA and derivative thermo-gravimetric (DTG) curves for GO, PS and nanocomposites are shown in figure 4 (a and b), respectively. All the curves showed a major weight loss between 100-300 °C. For GO, there was an initial weight loss of 4-5 % at room temperature attributed to buoyancy effects as the method included 5 minutes isotherm at 25 °C for gas purge before starting to increase the temperature. This step was important to flush the air out of the atmosphere before heating. The decomposition started from 180 °C due to the pyrolysis of unstable oxygenated functional groups attached to the graphene surface. Gas generation was associated with this drastic weight loss for GO including CO and CO<sub>2</sub> [38, 39].

The decomposition of PS started at around 120 °C and significant decomposition started at around 260 °C as observed from TGA measurements due to main chain pyrolysis. The maximum degradation temperature ( $T_d^{\text{peak}}$ ) of the nanocomposites increased from 347 °C for the neat polymer to 360.4 °C, and 361.5 °C for PS/GO and PS/GO D respectively. Nano-fillers



can cause a restriction to the mobilization of PS macromolecules. Furthermore, such range of higher degradation temperatures compared with the neat PS suggested a strong interaction between the matrix and the nano-fillers [40]. The improvement of the thermal stability of the nanocomposites compared to the neat polymer can also be ascribed to the jammed network of char layers formed by graphene based materials which could retards the transportation of the decomposed combustible chemicals [5]. The work done by some authors [41] studied the dispersion quality for an organophilic montmorillonite clay in the polymer matrix of poly(ethylene oxide) by using a sonication technique. The dispersion quality was better for the sonicated samples compared with non-sonicated ones. The thermal decomposition temperature was higher (327 °C) after using the sonication technique as an efficient processing factor, compared to that of the samples prepared without using sonication (311 °C).



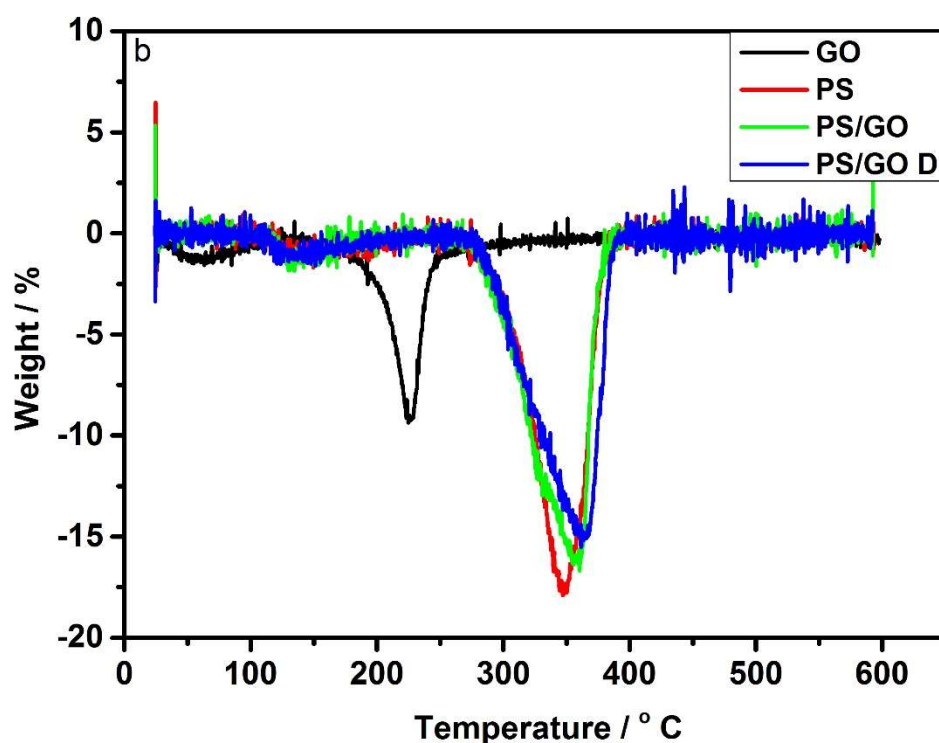


Figure 4: a- TGA and b- DTG inset curves for GO, PS and nanocomposites with different periods of mixing.

The DSC curves for the neat PS and the PS/GO nanocomposites that have the same weight fraction but different times of mixing are shown in figure 5. For each curve,  $T_g$  was calculated from the midpoint of the step change in the specific heat of each sample. It can be seen that the value of  $T_g$  increased for the nanocomposites compared with the neat polymer.  $T_g$  for PS was 99.4 °C whilst  $T_g$  for PS/GO was 103.0 °C and for PS/GO D was 104.4 °C. The increment in the value of  $T_g$  with the matrix reinforcement with GO nano-particles confirmed that the interfacial interaction between the matrix and the nano-particles was sufficiently strong to hinder the polymer chains movement at the interface [42]. A study [43] showed that sonication played a crucial role in disintegration of the agglomerates. It found that the use of the shear mixer for 2 minutes at 3000 rpm to mix the untreated carbon nanotubes with the polymer matrix led to an increase in  $T_g$ . This was related to the reduction of the mobility of the matrix molecules arising from strong interfacial interactions between the matrix and the nanotubes.



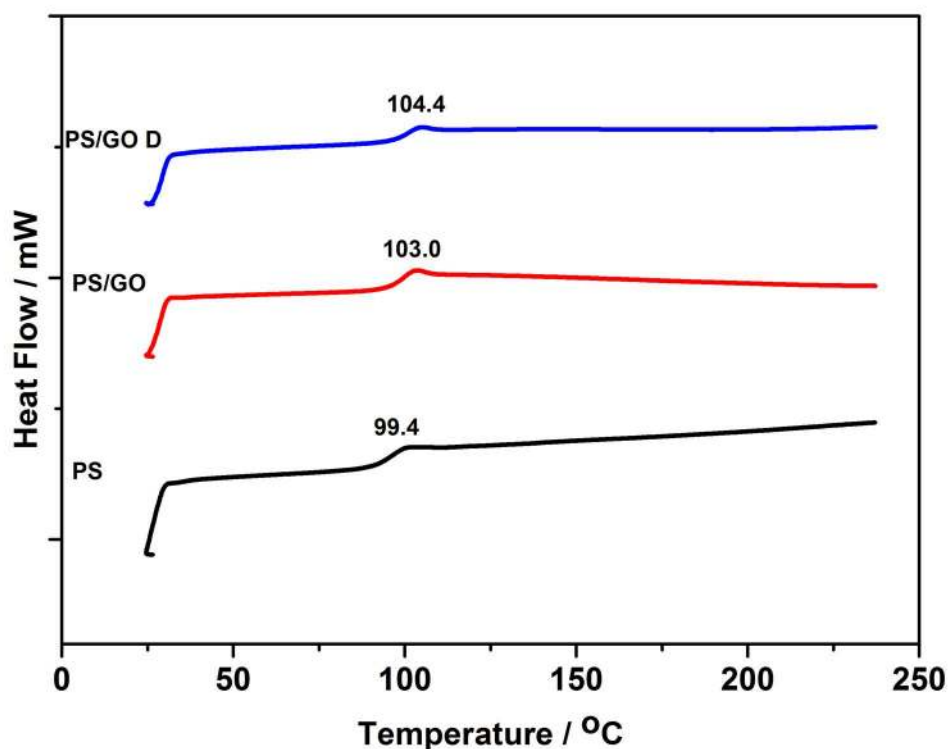


Figure 5:  $T_g$  values obtained by DSC for the pristine polymer and nanocomposites prepared by different periods of mixing.

Dynamic mechanical analysis was used to measure the viscoelastic properties for the materials. Figure 6a and 6b shows the variation of storage modulus and  $\tan \delta$  (ratio between the viscous part of the polymer to the elastic one) as a function of temperature for the polymer and nanocomposite materials using a single cantilever mode. It can be observed that the values of storage modulus for neat PS and its nanocomposites decreased as the temperature increased. This behaviour can be ascribed to the polymer chains movement with the increasing temperature. At a temperature of 30 °C, the storage modulus was 1.93 GPa for neat PS, 2.33 GPa for PS/GO, and 2.02 GPa for PS/GO D. The addition of GO to the polymer matrix led to significant improvements in storage modulus values at the glassy stage (30 °C) at which the polymeric molecules were frozen.

GO played a crucial role in the increment of the values of storage modulus due to the strong interfacial interaction between PS and the well dispersed nano-sheets of GO with high modulus [44]. The long period of mixing represented by PS/GO D showed lower values of storage modulus compared with those of neutral period of mixing represented by PS/GO. This result is similar to that found by a research group [45] who showed that 90 minutes of sonication for 0.2 wt. % of carbon nano-fibres in polyester gave a better value of storage modulus than 120 minutes of sonication. The aforementioned research group explained that this shorter level of sonication, rather than the longer one, facilitated a suitable dispersion without destroying the nano-fibres in ways such as buckling, bending, and breakage.

It is sometimes common to see humps and peaks on the storage modulus directly preceding to the drop of the curve with increasing temperature. These peaks or humps are associated with the re-arrangement in the molecule to relieve stresses frozen in below the  $T_g$  by the processing method. These stresses are trapped in the material until enough mobility is obtained at the  $T_g$  to permit the chains to move to a lower energy state [46].

Figure 6b shows a shift in values of  $T_g$  from around 91.0 °C for the neat PS to 107.2 °C for PS/GO, to around 107.6 °C for PS/GO D. The strong interfacial interaction between the matrix and the nano-filler is a result of high specific surface area and good dispersion of nano-particles in the matrix as found in the DSC measurements. All of the aforementioned results confirmed the occurrence of restrictions in the segmental movement of the polymer chains and a shift in  $T_g$  values [47,48].

It has been noticed that the values of  $T_g$  recorded by DMA are different to those ones recorded by DSC. The reason behind this can be ascribed to the sensitivity of DMA which is higher in the detection of glass transition than the case with DSC [46]. DMA can also resolve other kinds of localized transitions such as side chain movements.

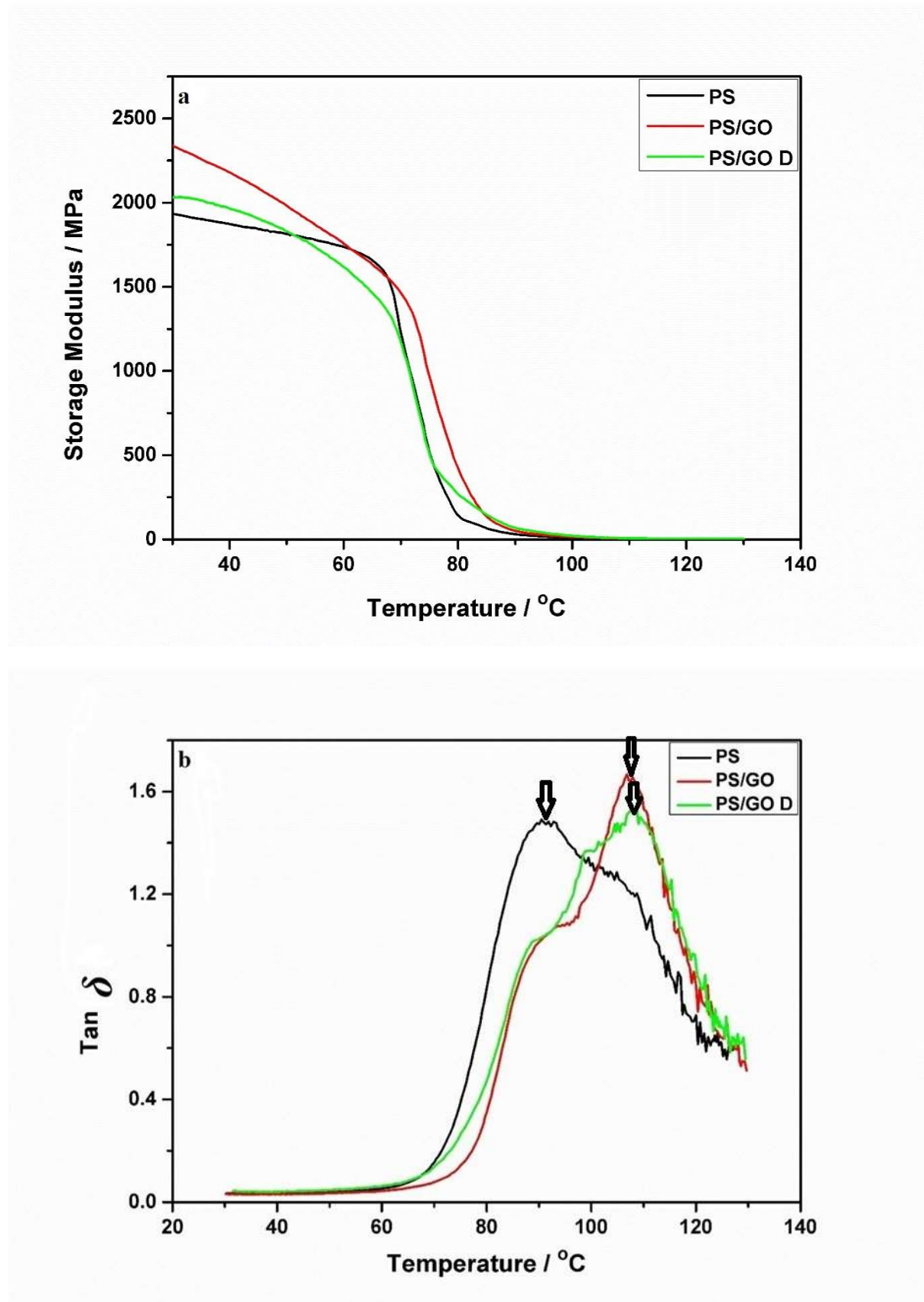


Figure 6: a- Storage modulus and b- Tan-δ for the polymer and the nanocomposites.

## Conclusions

In this study, the effect of dispersion condition of GO nano-sheets in PS was investigated. A optimal dispersion condition for synthesizing nanocomposites of GO nano-sheets embedded in a thermoplastic matrix of PS is concluded. The images of optical microscopy, SEM, and TEM confirmed a good distribution of the nano-sheets in the matrix using magnetic stirring, bath sonication, and shear mixing for both long and neutral time of mixing for the last two techniques. FTIR spectra of the nanocomposites did not show an obvious peak of GO due to the low weight fraction of GO employed in this study.

Although a good improvement was noticed for  $T_g$  values obtained by DSC for nanocomposites prepared by long-time of mixing, the results of storage modulus showed that the neutral time of mixing could prevent the nano-sheets from damage. Overall, the use of THF and both techniques of bath sonication and shear mixing as dispersion techniques led to enhancements in thermal and thermo-mechanical properties for PS/GO nanocomposites.

## Acknowledgements

Zaid G. Mohammadsalih would like to thank The Ministry of Higher Education and Scientific Research in The Republic of Iraq for granting the PhD scholarship. He would also like to thank The University of Technology, Applied Science Department, Applied Science Research Unit for their valuable support.

## References

- [1] Han, Y. et al., 2013. Preparation and properties of polystyrene nanocomposites with graphite oxide and graphene as flame retardants. *Journal of Materials Science*, 48(12), pp.4214–4222.

- [2] Dhand, V. et al., 2013. A Comprehensive Review of Graphene Nanocomposites: Research 219 Status and Trends. *Journal of Nanomaterials*, 2013, 763953.
- [3] Geim, A.K and Novoselov, K.S. 2007. The rise of graphene. *Nature Mater.*, 6(3), pp.183–191.
- [4] Singh, V. et al., 2011. Graphene based materials: Past, present and future. *Progress in Materials Science*, 56(8), pp.1178–1271.
- [5] Fan, W. and Zhang, C. 2013. Fabrication of electrically conductive graphene/polystyrene composites via a combination of latex and layer-by-layer assembly approaches. *Journal of Materials Research*, 28(4), pp.611–619.
- [6] Economopoulos, S.P. & Tagmatarchis, N., 2013. Chemical functionalization of exfoliated graphene. *Chemistry - A European Journal*, 19(39), pp.12930–12936.
- [7] Maheshkumar, K.V. et al., 2014. Research updates on Graphene oxide based polymeric nanocomposites. *Polymer Composites*, 35(12), pp. 2297–2310.
- [8] Krishnamoorthy, K. et al., 2013. The chemical and structural analysis of graphene oxide with different degrees of oxidation. *Carbon*, 53, pp.38–49.
- [9] Salavagione, H. J. et al., 2011. Graphene-based polymer nanocomposites. In *Physics and applications of graphene*. Edited by Mikhailov S. INTECH Europe, pp. 1–14.
- [10] Zhao, X. et al., 2010. Enhanced mechanical properties of graphene-based polyvinyl alcohol composites. *Macromolecules*, 43(5), pp.2357–2363.
- [11] Yasmin, A. et al., 2006. Processing of expanded graphite reinforced polymer nanocomposites. *Composites Science and Technology*, 66(9), pp.1182–1189.
- [12] Qiu, S. et al., 2015. Effect of functionalized graphene oxide with organophosphorus oligomer on the thermal and mechanical properties and fire safety of polystyrene. *Industrial and Engineering Chemistry Research*, 54(13), pp.3309–3319.
- [13] Johnson, D.W., Dobson, B.P. & Coleman, K.S., 2015. A manufacturing perspective on graphene dispersions. *Current Opinion in Colloid and Interface Science*, 20(5–6), pp.367–382.
- [14] Hasan, M. & Lee, M., 2014. Enhancement of the thermo-mechanical properties and efficacy of mixing technique in the preparation of graphene/PVC nanocomposites compared to carbon nanotubes/PVC. *Progress in Natural Science: Materials International*, 24(6), pp.579–587.
- [15] Chen, B and Evans, J. R.G., 2006. Nominal and Effective Volume Fractions in Polymer-Clay Nanocomposites. *Macromolecules*. 39, pp.1790-1796.
- [16] Verdejo, R. et al., 2011. Graphene filled polymer nanocomposites. *Journal of Materials Chemistry*, 21(10), pp.3301–3310.

- [17] Iqbal, M.Z. et al., 2016. Processable conductive graphene/polyethylene nanocomposites: Effects of graphene dispersion and polyethylene blending with oxidized polyethylene on rheology and microstructure. *Polymer*, 98, pp.143–155.
- [18] Tang, H. et al., 2012. Highly efficient synthesis of graphene nanocomposites. *Nano Letters*, 12(1), pp.84–90.
- [19] Layek, R.K. & Nandi, A.K., 2013. A review on synthesis and properties of polymer functionalized graphene. *Polymer*, 54(19), pp.5087–5103.
- [20] Xu, Z and Chao, G., 2011. Aqueous Liquid Crystals of graphene oxide. *American chemical society*. 5(4), pp. 2908-2915.
- [21] Ayán-Varela, M. et al., 2014. A quantitative analysis of the dispersion behavior of reduced graphene oxide in solvents. *Carbon*, 75, pp.390–400.
- [22] Peponi, L. et al. 2014. Processing of nanostructured polymers and advanced polymeric based nanocomposites. *Materials Science and Engineering R*, 85, pp. 1-46.
- [23] Chandrasekaran, S., Seidel, C. & Schulte, K., 2013. Preparation and characterization of graphite nano-platelet (GNP)/epoxy nano-composite: Mechanical, electrical and thermal properties. *European Polymer Journal*, 49(12), pp.3878–3888.
- [24] Prolongo, S.G. et al., 2008. Effects of dispersion techniques of carbon nanofibers on the thermo-physical properties of epoxy nanocomposites. *Composites Science and Technology*, 68(13), pp.2722–2730.
- [25] Cosmoiu, I. et al., 2016. Influence of Filler Dispersion on the Mechanical Properties of Nanocomposites. *Materials Today: Proceedings*, 3(4), pp.953–958.
- [26] Marcano, Daniela C. et al., 2010. Improved Synthesis of Graphene Oxide. *ACS Nano*, 4(8), pp.4806–4814.
- [27] Gupta, M.L. et al., 2013. The effect of mixing methods on the dispersion of carbon nanotubes during the solvent-free processing of multiwalled carbon nanotube/epoxy composites. *Journal of Polymer Science, Part B: Polymer Physics*, 51(6), pp.410–420.
- [28] Lowe, S.E and Zhong, Y.L., Challenges of Industrial-Scale Graphene Oxide Production in *Graphene Oxide Production. Graphene Oxide: Fundamentals and Applications*, 1<sup>st</sup> Edition. Edited by Dimiev A.M. and Eigler, John Wiley & Sons, Ltd. 2017.
- [29] Konios, D. et al., 2014. Dispersion behaviour of graphene oxide and reduced graphene oxide. *Journal of Colloid and Interface Science*, 430, pp.108–112.
- [30] Li, Z. et al., 2015. Improved synthesis of fluffy and wrinkled reduced graphene oxide for energy storage application. *Vacuum*, 117, pp.35–39.
- [31] Ionita, M. et al., 2014. Improving the thermal and mechanical properties of polysulfone by incorporation of graphene oxide. *Composites Part B: Engineering*, 59, pp.133–139.
- [32] Ming, R et al., 2013. Humidity-dependant compression properties of graphene oxide foams prepared by freeze-drying technique. *Micro & Nano Letters*, 8(2), pp.66–67.

- [33] Yin, G. et al., 2013. Preparation of graphene oxide coated polystyrene microspheres by Pickering emulsion polymerization. *Journal of colloid and interface science*, 394, pp.192–198.
- [34] Heo, C. et al., 2012. ABS nanocomposite films based on functionalized graphene sheets. *Journal of Applied Polymer Science*, 124(7), pp.4663–4670.
- [35] Wu, N. et al. 2015. Synthesis of network reduced graphene oxide in polystyrene matrix by a two-step reduction method for superior conductivity of the composites. *Journal of Materials Chemistry*, 22, pp. 17254-17261.
- [36] Ding, P. et al., 2015. Anisotropic thermal conductive properties of hot-pressed polystyrene/graphene composites in the through-plane and in-plane directions. *Composites Science and Technology*, 109, pp.25–31.
- [37] Vukoje, I.D. et al., 2014. Characterization of silver/polystyrene nanocomposites prepared by in situ bulk radical polymerization. *Materials Research Bulletin*, 49, pp.434–439.
- [38] El-Khodary, S. a. et al., 2014. Preparation and Characterization of Microwave Reduced Graphite Oxide for High-Performance Supercapacitors. *Electrochimica Acta*, 150, pp.269–278.
- [39] Tang, L.C. et al., 2014. Creep and recovery of polystyrene composites filled with graphene additives. *Composites Science and Technology*, 91, pp.63–70.
- [40] Lee, W. et al., 2013. Simultaneous enhancement of mechanical, electrical and thermal properties of graphene oxide paper by embedding dopamine. *Carbon*, 65, pp.296–304.
- [41] Lim, S.T. et al., 2003. Dispersion quality and rheological property of polymer clay NC ultrasonication effect. , 9(1), pp.51–57.
- [42] Wan, C. & Chen, B., 2012. Reinforcement and interphase of polymer/graphene oxide nanocomposites. *Journal of Materials Chemistry*, 22(8), pp.3637–3646.
- [43] Chen, H. et al., 2007. Effect of dispersion method on tribological properties of carbon nanotube reinforced epoxy resin composites. *Polymer Testing*, 26(3), pp.351–360.
- [44] Yu, Y.-H. et al., 2014. High-performance polystyrene/graphene-based nanocomposites with excellent anti-corrosion properties. *Polymer Chemistry*, 5(2), pp.535–550.
- [45] Hossain, M.E. et al., 2015. Effect of Dispersion Conditions on the Thermal and Mechanical Properties of Carbon Nanofiber–Polyester Nanocomposites. *Journal of Engineering Materials and Technology*, 137(3), pp.1–9.
- [46] Menard, K.P., *Dynamic Mechanical Analysis of Polymers and Rubbers*. in *Encyclopedia of Polymer Science and Technology*, Edited by Mark, H.F. John Wiley and Sons. 2015.
- [47] Hu, H. et al., 2010. Preparation and properties of graphene nanosheets-polystyrene nanocomposites via in situ emulsion polymerization. *Chemical Physics Letters*, 484(4–6), pp.247–253.

[48] Srivastava, R.K. et al., 2011. The strain sensing and thermal-mechanical behaviour of flexible multi-walled carbon nanotube/polystyrene composite films. *Carbon*, 49(12), pp.3928–3936.